1

Bracketing phenotypic limits of mammalian hybridization

3

4 Yoland Savriama[1]†, Mia Valtonen[1,2]†, Juhana Kammonen[3]†, Pasi Rastas[3], Olli-Pekka

5 Smolander[3], Annina Lyyski[3], Teemu J. Häkkinen[1], Ian J. Corfe[1], Sylvain Gerber[4], Isaac Salazar-

6 Ciudad[1,5], Lars Paulin[3], Liisa Holm[3,6], Ari Löytynoja[3]*, Petri Auvinen[3]*, Jukka Jernvall[1]*

7

8 [1]Developmental Biology Program, Institute of Biotechnology, University of Helsinki, P.O. Box

9 56, FIN-00014 Helsinki, Finland.

10 [2]Department of Environmental and Biological Sciences, University of Eastern Finland, P.O.

11 Box 111, FIN-80101 Joensuu, Finland.

12 [3]Genome Biology Program, Institute of Biotechnology, University of Helsinki, P.O. Box 56,

13 FIN-00014 Helsinki, Finland.

14 [4]Institut Systématique Evolution Biodiversité (ISYEB), Muséum national d'Histoire naturelle,

15 CNRS, Sorbonne Université, EPHE, 45 rue Buffon, CP 50, 75005 Paris, France.

16 [5]Departament de Genètica i Microbiologia, Universitat Autònoma de Barcelona, 08193

17 Cerdanyola del Vallès, Spain.

18 [6]Faculty of Biological and Environmental Sciences, University of Helsinki, P.O. Box 56, FIN-

19 00014 Helsinki, Finland.

20 †These authors contributed equally to this work.

21 *For correspondence: ari.loytynoja@helsinki.fi, petri.auvinen@helsinki.fi, or

22 jernvall@fastmail.fm.

23

Abstract

An increasing number of mammalian species have been shown to have a history of hybridization and introgression based on genetic analyses. Only relatively few fossils, however, preserve genetic material and morphology must be used to identify the species and determine whether morphologically intermediate fossils could represent hybrids. Because dental and cranial fossils are typically the key body parts studied in mammalian paleontology, here we bracket the potential for phenotypically extreme hybridizations by examining uniquely preserved cranio-dental material of a captive hybrid between gray and ringed seals. We analyzed how distinct these species are genetically and morphologically, how easy it is to identify the hybrids using morphology, and whether comparable hybridizations happen in the wild. We show that the genetic distance between these species is more than twice the modern human-Neanderthal distance, but still within that of morphologically similar species-pairs known to hybridize. In contrast, morphological and developmental analyses show gray and ringed seals to be highly disparate, and that the hybrid is a predictable intermediate. Genetic analyses of the parent populations reveal introgression in the wild, suggesting that gray-ringed seal hybridization is not limited to captivity. Taken together, gray and ringed seals appear to be in an adaptive radiation phase of evolution, showing large morphological differences relative to their comparatively modest genetic distance. Because morphological similarity does not always correlate with genetic distance in nature, we postulate that there is considerable potential for mammalian hybridization between phenotypically disparate taxa.

44

Introduction

Although hybridization has been extensively examined in the context of speciation, the role of interbreeding leading to introgression and admixture of phenotypic traits is attracting increasing attention (Ackermann et al., 2006; Mallet, 2007; Abbott et al., 2013; Polly et al., 2013; Pennisi, 2016; Árnason et al., 2018; Lamichhaney et al., 2018). In studies of human evolution, genetic

50 evidence has implicated introgression between different lineages of *Homo* (Green et al., 2010;

51 Meyer et al., 2012), and an increasing number of mammalian fossils are suggested to retain

52 signs of interbreeding by palaeogenomic studies (Enk et al., 2011; Fu et al., 2011; Wecek et al.,

53 2017). Hybridization can complicate the assignment of fossil specimens to specific taxa

54 (Trinkaus et al., 2003; Trinkaus, 2007; Polly et al., 2013; Martinón-Torres et al., 2017), and

55 currently it remains unclear how phenotypically different or disparate taxa might be expected to

56 hybridize. Even if hybrids between morphologically dissimilar species have reduced fertility,

57 they may still be preserved in the fossil record, especially if hybridization is fairly common as in

58 active hybrid zones (e.g., Mallet, 2007; Polly et al., 2013; Shurtliff, 2013; Pallares et al., 2016).

59 To assess the maximum morphological range of potential hybridization in the fossil record,

60 analyses of hybrids between morphologically disparate taxa are required. One such

61 hybridization, with uniquely preserved cranial material, has been reported to have occurred in

62 Stockholm zoo in 1929 between two mammalian species belonging to different genera; the gray

63 seal (*Halichoerus grypus*) and the ringed seal (*Pusa hispida*) (Lönnberg, 1929). This incident

64 raises questions as to how distinct these species are genetically, how distinct these species are

65 phenotypically, how easy it is to identify the hybrids using morphology, and whether

66 comparable hybridizations happen in the wild. Addressing all these questions together allows

67 one to estimate the 'hybrid bracket', or the overall potential for hybridization in mammalian

68 evolution.

69

70 **Results**

71 **Validating the seal hybrid and the genetic context of the hybridization.** The seal born in

72 1929 was immediately concluded to be a hybrid because at the time the seal pond housed only

73 three adult seals; two male gray seals and one female ringed seal (Figure 1). The newborn was

74 found dead and although no malformations were reported (Lönnberg, 1929), both biological and

75 husbandry related causes of death remain a possibility. First, to verify the hybridization and

76 validate the identity of the museum specimen, we sequenced its genome (see Materials and

77 Methods, Table supp. 1) together with the genomes of its parental species, Baltic gray seals ($n =$

78 10) and Baltic ringed seals ($n = 9$) (see Materials and Methods). A genetic admixture analysis

79 shows that the hybrid shares roughly 50% of its genome with both species, confirming that it is

80 indeed a hybrid between the gray and the ringed seal (Figure 1C).

81 The exact phylogenetic position and distinctiveness of the gray seal in relation to the

82 ringed seal and other related taxa has been problematic (Fulton and Strobeck, 2010; Nyakatura

83 and Bininda-Emonds, 2012; Berta et al., 2018), leaving open the question how genetically

84 distinct the species really are. To approximate the genetic context of the seal hybridization, we

85 computed a genome-wide estimate of neutral genetic distance between gray and ringed seals

86 (see Materials and Methods), and contrasted this with species pairs well known to hybridize;

87 lion-tiger (*Panthera leo–P. tigris*) and domestic donkey–horse (*Equus asinus–E. ferus*) (see

88 Materials and Methods, Table supp. 2). Lion and tigers readily hybridize in captivity (Vella et

89 al., 1999), and as both they and seals are members of Carnivora, provide an appropriate

90 comparison. Whereas these carnivoran species-contrasts have the same number of chromosomes

91 [2n = 32 in seals (Corfman and Richart, 1964; Árnason, 1970) and 2n = 38 in felids (Vella et al.,

92 1999)], donkey and horse differ in their chromosome number and their hybrids, known as mules

93 and hinnies, are generally infertile [2n = 62 in donkeys and 2n = 64 in horses (Jónsson et al.,

94 2014)]. To place the results in the context of *Homo* lineage, human and Neanderthal were also

95 included in the analysis, as were some additional outgroups (Table supp. 2).

96 To obtain a robust proxy of neutral sequence evolution, we used the fourfold degenerate

97 sites of 4,045 protein-coding genes, present as single copy in each species (see Materials and

98   Methods). Analyses of 623,391 fourfold degenerate sites from genes orthologous for all the

99   eight species show that the gray-ringed seal genetic distance is roughly 49% and 26% of the

100   lion-tiger and donkey-horse distances, respectively (Figure 2, Table 1). These distances appear

101   robust when larger or smaller sets of species are compared (Table supps 3, 4). The

102   comparatively short genetic distance between the gray and ringed seals is noteworthy because

103   unlike in the hybridizing lion-tiger and donkey-horse comparisons, the dental and cranial

104   morphologies of the two seal species have historically warranted a genus level distinction

105   (Fulton and Strobeck, 2010; Nyakatura and Bininda-Emonds, 2012; Berta et al., 2018) in

106   contrast to the species level distinctions of the lion-tiger and donkey-horse pairs.

107   Even though the gray-ringed seal genetic distance is shorter than the carnivore and

108   perissodactyl contrasts (Figure 2), it is still considerably longer than the hominin contrast.

109   Compared to the modern human-Neanderthal distance, the gray-ringed seal distance is roughly

110   two and a half times greater (258%, Table 1), suggesting that many fossil hominins are within

111   the genetic hybrid bracket. Since several of the potentially hybridizing hominins are also

112   phenotypically different, next we analyzed the dental and cranial distinctiveness of the two seal

113   species and their hybrid. These phenotypic structures are the key features in many

114   paleontological studies.

115

116   **Analyzing the teeth of the hybrid.** Mammalian tooth shape is fully formed prior to function

117   with no remodeling other than wear after mineralization, thereby providing relatively direct

118   information about development. In addition, seals have vestigial deciduous dentitions and are

119   born with an erupting permanent dentition. Even though the newborn hybrid was found dead,

120   the precocious state of seal dental development allows us to compare the hybrid with adult seals

121   (Figure 1C). The original description of the hybrid by Lönnberg (1929), while detailed, was not

122 quantitative and therefore we 3D-reconstructed the hybrid dentition from microCT scans (see

123 Materials and Methods, Figure 3A, Figure supp. 1). Here we focus on the lower postcanine

124 dentitions as they show the largest range of variation and have been studied previously

125 (Jernvall, 2000; Salazar-Ciudad and Jernvall, 2010). Whereas seal dentitions are relatively

126 derived from the basic carnivoran pattern, seal postcanine morphologies are reminiscent of

127 various pretribosphenic patterns in mammalian evolution, classified to different families and

128 orders (Luo, 2007; Grossnickle and Polly, 2013).

129   The overall morphologies of the gray and ringed seal postcanine teeth are markedly

130 different. Ringed seal teeth have three to five slender cusps, and the teeth are generally more

131 similar along the jaw (Figure 1B, Figure 3A, Table supp. 5). In contrast, especially the anterior

132 postcanine teeth of the gray seal have large, fang-shaped central cusps with small, variably

133 present accessory cusps (Figure 1B, Figure 3A, Table supp. 5). These morphological differences

134 reflect the use of smaller fish and invertebrate foods by ringed seals compared to gray seals that,

135 in addition to fish are known to prey on mammals (Stringell et al., 2015; van Neer et al., 2015).

136 Because standard morphometric methods cannot be effectively used to compare teeth with

137 different numbers of tooth cusps, we quantified the shapes by using a top-cusp angle, a measure

138 of relative cusp height used previously in the analyses of seal dentitions (see Materials and

139 Methods) (Jernvall, 2000; Salazar-Ciudad and Jernvall, 2010).

140   The results show that the hybrid teeth are intermediate between a sample (n = 130) of the

141 parent species by having relatively large central cusps, but also relatively prominent accessory

142 cusps (Figure 3A, Figure supp. 2). The distinct and intermediate morphology of the hybrid is

143 most readily visible in the anterior postcanines (P2 and P3) in which the species differences are

144 also the greatest due to the stronger anteroposterior gradation in the gray seal dentition (Figure

145 3A, B, Figure supp. 2). In addition to shape, tooth size also appears intermediate between the

146   gray and ringed seal (Figure 3A). Because of the intermediate cusp morphologies of the hybrid,

147   next we examined what kind of developmental changes might drive the observed patterns.

148

149   **Developmental basis of the hybrid teeth.** Genetic regulation of mammalian tooth development

150   is highly conserved (Jernvall and Thesleff, 2012), and reiterative activation of signaling centers,

151   called secondary enamel knots, appear to direct cusp development in all studied mammals

152   (Jernvall and Thesleff, 2012). Consequently, computational modeling of genetic interactions

153   and tissue biomechanics, based on empirical data on mouse tooth development, has been used to

154   model embryological development of the teeth of rodent species (Harjunmaa et al., 2014;

155   Renvoisé et al., 2017), as well as seal teeth (Salazar-Ciudad and Jernvall, 2010). Since neither

156   seal tooth development nor hybridization is amenable to experimentation, we examined whether

157   the hybrid morphology could be produced by modeling development.

158   First, we generated virtual ringed and gray seal tooth rows (using real population mean

159   shapes, see Materials and Methods) using the ToothMaker-software (Harjunmaa et al., 2014;

160   Renvoisé et al., 2017) (see Materials and Methods). Setting three model parameters to different

161   values was sufficient to model the differences between gray and ringed seal teeth; inhibitor

162   (*Inh*), epithelial growth rate (*Egr*), and anterior bias (*Abi*). These parameters, by regulating the

163   dynamics of development, affect the spacing of cusps, the pointedness of cusps, and the

164   anterior-posterior symmetry of teeth, respectively (Figure supp. 3A, see Materials and

165   Methods). Changes along the tooth row were produced by a constant change in *Egr* in ringed

166   seal models and a constant change in *Egr* and *Inh* in gray seal models (Table supp. 6, see

167   Materials and Methods). The constant parameter changes not only parsimoniously account for

168   well recognized gradual shape changes along the tooth row (Butler, 1939; Van Valen, 1962;

169   Bateson, 1984), but also agree with the inhibitory cascade model that predicts a constant change

170   in tooth size proportions along the jaw (Kavanagh et al., 2007).

171   To mimic the hybridization between gray and ringed seals, the development of each tooth

172   along the jaw was simulated after adjusting each of the three parameters separating the two

173   species. For each parameter we used either the average parameter value (assuming no

174   dominance) or value adjusted 10% towards each of the parents. Additionally, we simulated teeth

175   by keeping one or two of the parameters at the parent values. We then simulated tooth

176   development using all these parameter value combinations (see Materials and Methods, Figure

177   supp. 3B, Table supps 6–8).

178   The resulting simulated tooth shapes show that the hybrid cusp patterns can be produced

179   by averaging the three parameters between the modeled gray and ringed seals (Figure 3C).

180   Furthermore, the top-cusp angles of this simulated hybrid tooth row fall between the parent

181   shapes similarly to the real hybrid (Figure 3D, Figure supp. 3B, Table supps 7, 8), suggesting

182   that the regulatory principles of tooth shape are largely conserved between the two seal species.

183   A key parameter differentiating the gray and ringed seal teeth that is also required to be

184   closest to the average between the parents is the inhibitor (*Inh*), as otherwise the simulated

185   hybrid would have the top-cusp angle close to one of the parents (Figure 3D, Table supps 7, 8,

186   Figure supp. 3B). Experiments on developing mouse teeth have identified sonic hedgehog

187   (SHH) as one candidate molecule for inhibition of new enamel knots and cusps (Harjunmaa et

188   al., 2014). However, because cusp spacing can be altered by tinkering with the activator-

189   inhibitor balance of enamel knots through several molecules, these results do not necessarily

190   implicate a single gene underlying each parameter. Rather, regardless of whether tooth shape is

191   driven by a large number of loci or relatively few loci with major phenotypic effects (for

192   discussion, see Pallares et al., 2016), our simulation results are strongly suggestive that the

193   hybrid dentition is both phenotypically and developmentally a predictable intermediate between

194   the species.

195

196   **Analyzing the cranium of the hybrid.** Unlike the dentition, the cranium of the newborn hybrid

197   does not allow direct comparison to adult seals. However, differences in cranium morphology

198   can be compared using geometric morphometrics across species and age groups (Klingenberg,

199   2010), and we digitized 46 3D-landmarks from newborn to adult gray and ringed seals (Figure

200   supp. 4, Table supp. 9, $n = 116$, Movie supp. 1, see Materials and Methods) to depict overall

201   changes in skull shape.

202   The results show that gray and ringed seal crania have distinct developmental trajectories,

203   and the newborn crania from each species are already well separated in the morphospace with

204   no overlap ($p < 0.0001$, permutation test on Procrustes distance with 10,000 rounds, Figure 4).

205   The hybrid cranium is positioned between the two species, and in the proximity of the geometric

206   morphometric mean of newborn gray and ringed seals (Figure 4). Therefore, as is the case for

207   the dentition, the overall morphology of the cranium appears to be an intermediate between the

208   species, a result agreeing with recent results on hybrids between different mouse strains (Warren

209   et al., 2018).

210   Examining the details of cranial shape shows that the first two principal components

211   distinguish features that separate the two species (explaining 61.6% of total variance) while the

212   third component captures some mixed traits common to both of them (explaining 7.5% of total

213   variance) (Figure supp. 5A). The hybrid differs from the geometric intermediate by having a

214   shorter snout, narrower zygomatic arches and a more elongated braincase (Figure supp. 5B, C),

215   agreeing with the original description reporting that some details of the hybrid cranial

216   morphology are closer to one, or the other species (Lönnberg, 1929). We note, however, that the

217   actual parents of the hybrid are not preserved, and thus some details of the morphology could

218   represent one of the individual parents. Another factor affecting cranial shape is pronounced

219   sexual dimorphism present in gray seals but not in ringed seals (Figure 4), although we did not

220   detect dimorphism in newborn crania ($p = 0.485$ for gray seals and $p = 0.839$ for ringed seals,

221   permutation tests on Procrustes distances with 10,000 rounds). Overall, the intermediate cranial

222   and dental features of the seal hybrid analyzed suggest that a perfectly intermediate fossil

223   specimen between two genera could potentially be a hybrid.

224

225   **Detecting hybridization in the wild.** Finally, because the grey-ringed seal hybrid was born in

226   captivity, in itself it does not imply that comparable hybridizations happen in the wild.

227   However, as is the case for mammals in general (Polly et al. 2013; Shurtliff, 2013; Árnason et

228   al., 2018; Warren et al., 2018), several seal species are well established as hybridising in the

229   wild, including documentation of fertile intergeneric hybrids (Franco-Trecu et al., 2016), and a

230   living intergeneric hybrid between the dentally disparate harp seal (*Pagophilus groenlandicus*)

231   and hooded seal (*Cystophora cristata*) (Kovacs et al., 1997). Furthermore, behavioural

232   observations have documented attempted matings by a wild gray seal male with harbour seal

233   females (*Phoca vitulina*) (Wilson, 1975).

234   To estimate potential interbreeding in the history of wild gray and ringed seals, we

235   examined introgression using the Patterson's D-statistics approach (Green et al., 2010). In

236   addition to Baltic gray seals and Baltic ringed seals, we sequenced genome wide data from

237   Saimaa ringed seals ($n = 12$, the Weddell seal was the outgroup, see Materials and Methods).

238   Saimaa ringed seals are a suitable contrast for the analyses (Figure 5A) because they have been

239   isolated from the Baltic for approximately 9,500 years, with no documented presence of gray

240   seals in Lake Saimaa (Valtonen et al., 2012; Ukkonen et al., 2014). The results show that Baltic

241   ringed seals have a statistically significant excess of derived alleles shared with the gray seal

242   compared to the Saimaa ringed seals (Figure 5B, Table supp. 10). We consider these results to

243   be at least suggestive of interbreeding occurring in the Baltic between gray and ringed seals, and

244   it is plausible that many seal populations and species will exhibit gene flow comparable to that

245   in bears (Kumar et al., 2017) and horses (Jónsson et al., 2014). Taken together, the captive gray-

246   ringed seal specimen can be considered to be a representative example of a phenotypically

247   disparate hybridization.

248

Discussion

250   Gray and ringed seals have sufficiently morphologically different dentitions that, if they were to

251   be discovered as unknown fossils, at least a genus level distinction could easily be justified. Yet,

252   the combination of our genomic, phenomic, and developmental, analyzes show that these

253   species can, and are likely to hybridize and that the resulting phenotype is a predictable

254   combination of the two species. In more general terms, this hybrid bracket is indicative of the

255   conservation of developmental mechanisms that tinker with quantitative traits. Whereas the

256   overall conservation of developmental signaling in tooth development across the whole of jawed

257   vertebrates is well established (Fraser et al., 2009; Jernvall and Thesleff, 2012), our results

258   suggest interspecies and higher level conservation of the regulatory architecture underlying

259   dental form. Previous reports have found increased occurrences of supernumerary teeth in

260   mammalian hybrids (Goodwin, 1998; Ackermann et al., 2006), which could indicate that there

261   is a point of divergence at which the developmental regulation begins to lose canalization. Loss

262   of developmental regulation underlying extra teeth is supported by the frequent presence of

263   supernumerary teeth in mice with null mutations affecting tooth development (Jernvall and

264   Thesleff, 2012). Supernumerary teeth are relatively common in seal populations (Cruwys and

265   Friday, 2006; Miller et al. 2007), but these are usually attributed to relaxed selection due to the

266   lack of refined occlusion in seals (Cruwys and Friday, 2006; Miller et al. 2007; Jernvall and

267   Thesleff, 2012). The potential role of interbreeding in the occurrence of extra teeth in seals

268   remains to be determined.

269   In the case of paleontological research where phenotypic analyses are the basis for

270   taxonomic inferences, our results suggest that many closely related genera could potentially

271   hybridize, and that intermediates between distinct species may be hybrids themselves. The large

272   morphological differences relative to the relatively modest genetic distance between gray and

273   ringed seals are suggestive of an adaptive radiation phase of evolution, and we postulate that

274   phenotypically disparate hybridizations are most likely to be observed in such radiations. In

275   itself, hybridization between species has been also proposed to facilitate adaptive radiations

276   (Seehausen, 2004; Warren et al., 2018). Finally, in our case, the hybrid seal was of the first

277   generation, and continuing interbreeding would result in segregation of traits, something that

278   might appear as a mosaic mixture of traits in the fossil record (Warren et al., 2018). With

279   advancing understanding of the developmental basis of organ form, it may be possible to

280   provide predictions of potential hybrids, even in cases where the phenotypic differences are

281   substantial.

282

Materials and Methods

284   **Specimen preparation.** The hybrid was a newborn and although the crown morphogenesis of

285   the permanent teeth was completed, the teeth were erupting and only partially mineralized. Seal

286   deciduous dentition is vestigial. The right side dentition was removed from the jaw by Lönnberg

287   (1929), and most of the teeth were cracked or split into halves during storage. The skull, jaws

288   and isolated teeth were microCT scanned using a custom-built microtomography system

289   (Nanotom 180 NF, phoenix|X-ray System and Service GmbH, General Electric, Wunstorf,

290   Germany) at the Department of Physics, University of Helsinki, Finland. The voxel size was

291   32.1 µm for the skull and 16.6 µm for the tooth row. Volume data were processed in Avizo 9.0

292   (FEI Visualization Sciences Group) and surfaces were extracted and teeth segmented from the

293   jaw using Artec Studio 9.0 (Artec 3D). Cracked tooth halves were manually reattached using

294   Artec Studio 9.0. The tooth halves were joined together without deforming the meshes (Figure

295   supp. 1). Skull images and drawings are from specimens in Finnish Museum of Natural History

296   (Helsinki, Finland) and partly for *Homo* from (Tattersall and Schwartz, 1998).

297

298   **Seal genetic data.** Hybrid DNA was isolated from the pulpa of a poscanine tooth that had fallen

299   from the specimen in storage using NucleoMag kit (Macherey-Nagel GmbH & Co, Germany).

300   The same method was used to isolate DNA from Baltic gray seal, Baltic ringed, and Saimaa

301   ringed seal muscle tissue samples. The Baltic seal samples were obtained from the collections of

302   the Saimaa Ringed Seal Genome Project, University of Helsinki, and Natural Resources

303   Institute Finland, whereas the Saimaa samples originated from the collections of the University

304   of Eastern Finland, which has a permission from Finnish environmental authorities for taking

305   possession of and storing tissues of the Saimaa ringed seal (permission number: Dnro

306   VARELY/3480/2016). All libraries and sequencing were performed at the DNA Sequencing

307   and Genomics Laboratory, Institute of Biotechnology, University of Helsinki, Finland. The

308   hybrid seal genome was sequenced with 2 separate runs of Illumina HiScanSQ platform and 11

309   separate runs of Illumina MiSeq platform to ca. 100X raw sequencing coverage (Table supp. 1).

310   The base calls in the Illumina HiScanSQ platform were converted into text format (FASTA-

311   format with individual base quality scores) using the CASAVA toolkit (bcl2fastq version 1.8.3)

312   provided by the manufacturer. The Illumina MiSeq platform employed a primary analysis

313   software called MiSeq Reporter post-run that produced the base calls in text format.

314   For all the Illumina reads, base call accuracy and read length filtering (adapter cutoff) was

315   performed with cutadapt (Martin, 2011) using minimum accepted base call accuracy of 90% and

316   minimum post-filtering read length of 75 bp. The Weddell seal (*Leptonychotes weddellii*) draft

317   genome (Broad Institute) was used as a reference genome for the downstream genetic distances

318   analysis. The statistics and downloads for this reference are available at:

319   http://software.broadinstitute.org/allpaths-lg/blog/?p=647.

320

321   **Admixture and introgression analyses.** Short read data for Hybrid, Baltic gray seal, Baltic

322   ringed seal, and Saimaa ringed seal were mapped to the Weddell seal reference genome.

323   Similarly, the reference Weddell seal individual's short read data was mapped to its reference

324   genome. The mapping was conducted using bwa mem (v. 0.7.15), samtools rmdup (v. 1.3.1) and

325   GATK IndelRealigner (v. 3.7). The resulting bam files were used for introgression and

326   admixture analyses.

327   To examine the hybrid, an admixture analysis was carried using NgsAdmix (Skotte et al.,

328   2013) and the pipeline at: http://www.popgen.dk/software/index.php/NgsAdmix. To reduce

329   computational burden, a random sample of 3.6 million markers (10% of the data) were used to

330   reduce the computation burden. NgsAdmix was run 10 times with K=2 clusters on the hybrid,

331   gray and ringed seals. Each of these runs converged to identical clustering.

332   Introgression was studied using Patterson's D-statistics (Green et al., 2010) that, other

333   than requiring the ancestral population to be randomly mating, is robust to variables such as

334   variations in population size (Durand et al., 2011). D-statistics was calculated by abbababa2

335   module of ANGSD (Korneliussen et al., 2014) using the first 1,000 scaffolds of the Weddell

336   genome (over 50% of the genome) and the default pipeline at:

337   http://www.popgen.dk/angsd/index.php/Abbababa2. To examine individual differences, the D-

338   statistics were calculated for each Baltic individual in addition to the Baltic sample. The Saimaa

339   ringed seals were set as P1, Baltic ringed seals as P2, and Baltic gray seals as P3. The aligned

340   sequences are available through the European Nucleotide Archive under accession number

341   PRJEB25679.

342

343   **Genetic distances.** To obtain a relatively robust and comparable measure of genetic distances

344   between the hybridizing species pairs, we analyzed fourfold degenerate (ffd) sites from a large

345   number of orthologous genes. As substitutions on ffd sites do not alter the encoded amino acid,

346   they can be considered a proxy of the neutral evolutionary process and thus be relatively free of

347   biases due to selection. A list of single-copy human genes and their orthologs in cat, dog, horse

348   and chimpanzee were fetched from Ensembl BioMart (v. 83) (Kinsella et al., 2011). 4,826

349   complete gene sets with unambiguous orthology ("Homology Type" is "ortholog_one2one";

350   "Orthology confidence" is "high") were retained and, for each reference species, nucleotide and

351   peptide sequences of every transcript were fetched using the Ensembl REST API (Yates et al.,

352   2014). Using last (v. 658) (Kiełbasa et al., 2011), scaffold-level genome assemblies of tiger,

353   Weddell seal and donkey were aligned against the genomes of cat, dog and horse, respectively.

354   Lift-over chains were built using the Kent source utilities (Kent et al., 2002). Short read data for

355   donkey and lion were mapped to the horse and tiger genomes using bwa mem (v. 0.7.15),

356   samtools rmdup (v. 1.3.1) and GATK IndelRealigner (v. 3.7) (Li and Durbin, 2009; McKenna et

357   al., 2010). Locally generated short read data for Baltic gray seal and Baltic ringed seal were

358   mapped to the Weddell seal genome. The data for the Neanderthal human individual were

359   obtained as bam alignment files. Data sources are listed in Table supp. 2.

360   The gene annotations were divided into individual coding exons, removing split codons

361   where necessary, and the exon coordinates in reference species (human, cat, dog, horse) were

362   transferred to related non-reference genomes using CrossMap (v. 0.2.4) (Zhao et al., 2013). For

363   each gene transcript, exons were independently extracted from the non-reference genomes using

364   samtools (v. 1.3.1) and matched against the reference peptide sequences using Pagan's (v. 0.61)

365   (Löytynoja et al., 2012) translated pileup alignment. The resulting back-translated nucleotide

366   alignments were flattened and degapped, combining all successfully extracted exons into one

367   sequence. For species with bam alignment data (donkey, gray and ringed seal, Neanderthal), the

368   genome regions surrounding the exons were reconstructed by placing observed sequence

369   changes to the genome sequences of horse, Weddell seal and human. For each exon separately,

370   variants were inferred with samtools mpileup and bcftools call (v. 1.3.1), and then placed to the

371   genome sequences with vcfutils vcf2fq, requiring sequencing depth of 10 or higher. The exon

372   regions of each transcript were extracted and combined into one sequence.

373   Sequence data were obtained for 4,329 genes. These sequences were aligned, selecting the

374   longest transcripts, with Pagan's translated pileup alignment. To remove artefacts of low quality

375   sequence (for example, due to assembly errors), resulting multiple sequence alignments were

376   filtered and regions where two neighboring codons contain more than one non-identical base

377   among all the study species were masked. For different species sets, gene sequence alignments

378   of at least 100 columns in length after filtering and removal of sites with missing data were

379   concatenated, and ffd sites were extracted using R package rphast (v. 1.6.5) (Hubisz et al.,

380   2010). Pairwise genetic distances were computed using R package ape (v. 4.0) (Paradis et al.,

381   2004) and model T92, and phylogenetic trees (Figure 2B) inferred with RAxML (v. 8.2.9)

382   (Stamatakis, 2006) using model GTRGAMMA. In addition, we measured the distances using all

383   the codon third sites, and the relative distances remained largely the same.

384   The species set analyzed are: all twelve species, eight species known to hybridize, the two

385   seals with each pair of hybridizing species. The numbers of input genes, codons and ffd sites as

386   well as the pairwise genetic distances for different species sets are given in Table 1 and Tables

387   supp. 3, 4.

388

389   **Dental material and analyses.** Baltic gray and ringed seal material was used in comparisons to

390   the hybrid as the parents were reported to be from the Baltic Sea (Dataset supp. 1, Table supp.

391   5). Postcanine teeth of seals are laterally compressed resembling early mammalian

392   morphologies, and the lateral views capture most of the shape variation (Jernvall, 2000). Images

393   were taken from the lingual views from a distance (approximately ten times the length of the

394   tooth row) and the number of cusps and top-cusp angles were tabulated using ImageJ (version

395   1.51). The angle captures the relative height of the tallest cusp, and correlates with cusp number

396   because cusp spacing and number are developmentally linked (Jernvall, 2000; Salazar-Ciudad

397   and Jernvall, 2010). For teeth that had only one or two cusps, the line was drawn to the

398   maximum anterior or distal ends at the crown base. We tabulated the presence of all cusps,

399   including small incipient cusplets (arrowheads in Figure supp. 1B). All the measurements

400   reported are from the right side. The pattern of results remains the same for the left side. Of the

401   65 gray and 65 ringed seal jaws studied, angle measurements were excluded from teeth with

402   substantially cracked or worn cusp tips. We also excluded jaws with anomalies such as extra

403   teeth. A sample of gray and ringed seal teeth were imaged twice and measured to confirm the

404   robustness of the angle measurements (mean absolute error = 1.0 and 1.5, SD = 0.92 and 1.08, n

405   = 40 and 46 teeth for gray and ringed seals, respectively). To test how intermediate the hybrid is

406   between the species, we calculated average top-cusp angles between each gray-ringed seal pair,

407   and tabulated the probability of obtaining the hybrid value from the gray-ringed seal averages

408   (Figure 3B, Figure supp. 2). For visualization, dental specimens were scanned with PlanScan

409   laser scanner (PlanMeca, Helsinki, Finland).

410

411   **Developmental modeling of teeth.** We used ToothMaker (Harjunmaa et al., 2014) to simulate

412   seal tooth development. The model integrates experimentally inferred genetic interactions with

413   tissue biomechanics to simulate tooth development (Salazar-Ciudad and Jernvall, 2010), and

414   here we used a version that had been experimentally explored in connection with mouse and

415   vole molar development (Harjunmaa et al., 2014; Renvoisé et al., 2017). We focused on three

416   parameters to simulate development of seal dentitions. To regulate spacing of cusps, the key

417   difference between gray and ringed seals, we adjusted the strength of the enamel knot-secreted

418   inhibition of enamel knot formation (parameter *Inh*). Experimental evidence on mouse molar

419   development has shown how adjusting inhibition of new enamel knots results in quantitative

420   changes in cusp spacing (Harjunmaa et al., 2014). Another strategy to alter cusp initiation would

421   be to adjust the activator (Harjunmaa et al., 2012), but here we prefer the inhibitor due to the

422   experimental data (Harjunmaa et al., 2012; 2014), and because increasing inhibition alone,

423   which leads to larger spacing of cusps as in the gray seal, does not inhibit growth directly (only

424   indirectly by inhibiting new enamel knots). The other two parameters used to simulate the

425   species differences are epithelial growth (*Egr*) and anterior bias (*Abi*). Egr affects the relative

426   growth of the epithelium and pointedness of cusps, and Abi the anterior extension of the tooth

427   germ; both have been found previously to account for variation in species differences (Salazar-

428   Ciudad and Jernvall, 2010; Harjunmaa et al., 2014; Renvoisé et al., 2017). Lateral biases (*Lbi*

429   and *Bbi*) affect lateral expansion of the tooth and indirectly cusp position laterally (Renvoisé et

430   al., 2017). Because seals have laterally compressed teeth, these parameters were kept constant.

431   One candidate gene for the lack of lateral expansion in seals is a transcription factor Foxi3

432   (Jussila et al., 2015), as *Foxi3* haploinsufficient dogs have seal like lower molars (Kupczik et

433   al., 2017). All the used parameter values are listed in the Table supp. 6. Top-cusp angle

434   measurements were done using ToothMaker and manually (Figure supp. 3B). We modeled gray

435 and ringed seal tooth rows by making constant parameter changes from tooth-to-tooth to mimic

436 gradual shape changes along the jaw. All the simulations were run for the same number of

437 iterations.

438   To simulate hybridization, for each tooth, we averaged the parameter values between the

439 species, adjusted the averages 10% towards each of the parents, or used the gray or ringed seal

440 value in different combinations (Figure supp. 3B, Table supp. 7). These different combinations

441 basically simulate how additively the parameters function, but do not imply that each parameter

442 would have one underlying locus. Rather, we consider the simulations to approximate the

443 overall developmental effect of the genetic backgrounds. ToothMaker software, is freely

444 available for Windows, MacOS, and Linux (available from the authors and with default seal

445 parameters at https://github.com/jernvall-lab/ToothMaker).

446

447 **Analysis of the crania**. 31 ventral and 22 dorsal 3D landmark coordinates were acquired from

448 skulls of complete ontogenetic series (from newborns to adults) of gray and ringed seals from

449 the collections of Finnish Museum of Natural History (Helsinki, Finland) using a Microscribe

450 G2X digitiser with 0.2 mm accuracy (Immersion). These data were merged together into a full

451 configuration of 46 landmarks using FileConverter (Klingenberg, 2011) (Figure supp. 4).

452 Digitizing was performed twice and one-way ANOVAs were used to test for digitizing error

453 (Table supp. 9). We analysed variation among individuals (symmetric component of variation)

454 apart from asymmetry (differences between left and right sides of individuals) (Savriama and

455 Klingenberg, 2011). A Generalized Procrustes Analysis (GPA) was used to simultaneously

456 superimpose all configurations and extract shape data by removing the effects of scale,

457 orientation and position (Klingenberg, 2010). Centroid size, the measure of size in geometric

458 morphometrics, was computed as the square root of the sum of the squared distances of all

459 landmarks from their centroid (Dryden and Mardia, 2016). Permutation tests were used for

460 testing differences in mean shapes using function 'permudist' from 'Morpho' R package

461 (Schlager, 2017).

462 A Principal Component Analysis (PCA) performed on the covariance matrix of shape variables

463 was used to show the main patterns of morphological variation between the two species. A 3D

464 microCT-scan of the hybrid was warped to the consensus using the Thin Plate Spline (TPS)

465 method via the function 'warpRefMesh' in Geomorph (Adams et al., 2017) and the main

466 patterns of shape changes were visualised as deviations from this warped consensus for the first

467 three principal components (PCs) (Figure supp. 5A). The hybrid was compared to the geometric

468 morphometric mean and differences were visualised via warping and heatmaps (Figure supp. 5B

469 and C). A multivariate quadratic regression of shape onto centroid size was used to investigate

470 the main patterns of allometric growth for each species that were visualised with warped 3D

471 microCT-scans of a newborn gray and ringed seal using Landmark Editor 3.6 and function

472 'warpmovie3d' (Figure 5, Movie supp. 1) (Wiley et al., 2005; Gerber and Hopkins, 2011;

473 Schlager, 2017). All analyses were performed with MorphoJ 1.06d (Klingenberg, 2011), custom

474 R (R Core Team, 2009) and Python scripts.

475

483   Muszynski for tomography and 3D data processing. We also thank P. Timonen and S. Oksanen

484   for help with Baltic seal samples. We thank CSC-IT Center for Science, Espoo, Finland, for

485   computing facilities. The personnel at DNA Sequencing and Genomics Laboratory, Institute of

486   Biotechnology, University of Helsinki is acknowledged for excellent technical work. We thank

487   PlanMeca corporation for equipment loan. We also thank Natural Resources Finland for

488   providing samples and Metsähallitus Parks & Wildlife Finland for co-operation. Key financial

489   support was provided by Jane and Aatos Erkko foundation and the Academy of Finland.

490

491   **Author Contributions:** J.J. and P.A. conceived the project, I.J.C. identified and Y.S.

492   reconstructed the hybrid specimen, P.A. sampled DNA from the hybrid, M.V. collected and

493   M.V. and J.J. analyzed dental data, T.J.H., I.S.-C. and J.J. performed the developmental

494   simulation, Y.S. collected and analysed cranial data, S.G. performed the allometric analyses for

495   cranial data, J.K, O.-P.S., A. Lyyski, L.P., and P.A. performed the sequencing and J.K., O.-P.S,

496   and L.H. the processing of the reads, A.L. analyzed genetic distances, and P.R. and A.L.

497   analyzed introgression. J.J. wrote the initial manuscript and all authors discussed the results and

498   provided input and scientific interpretations on the manuscript.

499   **Data and materials availability:** The aligned sequences are available through the European

500   Nucleotide Archive under accession number PRJEBxxxxx with individual sample accessions

501   (xxx...xxx). The cranial specimens listed in this study are archived in the Finnish Museum of

502   Natural History and Swedish Museum of Natural History. Any further data not available in the

503   Supporting Materials are available from the corresponding authors on request.

504

505   **References**

506 R. J. Abbott, D. Albach, S. Ansell, J. W. Arntzen, S. J. E. Baird, N. Bierne, J. Boughman, A.
507   Brelsford, C. A. Buerkle, R. Buggs, R. K. Butlin, U. Dieckmann, F. Eroukhmanoff, A.
508   Grill, S. H. Cahan, J. S. Hermansen, G. Hewitt, A. G. Hudson, C. Jiggins, J. Jones, B.
509   Keller, T. Marczewski, J. Mallet, P. Martinez‑Rodriguez, M. Möst, S. Mullen, R. Nichols,
510   A. W. Nolte, C. Parisod, K. Pfennig, A. M. Rice, M. G. Ritchie, B. Seifert, C. M. Smadja,
511   R. Stelkens, J. M. Szymura, R. Väinölä, J. B. W. Wolf, D. Zinner, Hybridization and
512   speciation. *J. Evol. Biol.* **26**, 229–246 (2013).

513 R. R. Ackermann, J. Rogers, J. M. Cheverud, Identifying the morphological signatures of
514   hybridization in primate and human evolution. *J. Hum. Evol.* **51**, 632–645 (2006).

515 D. C. Adams, M. L. Collyer, A. Kaliontzopoulou, E. Sherratt (2017) *Geomorph: Software for*
516   *geometric morphometric analyses. R package version 3.0.5,* https://cran.r-
517   project.org/package=geomorph.

518 Ú. Árnason, The karyotype of the gray seal (*Halichoerus grypus*). *Hereditas* **64,** 237–242
519   (1970).

520 Ú. Árnason, F. Lammers, V. Kumar, M. A. Nilsson, A. Janke, Whole-genome sequencing of the
521   blue whale and other rorquals finds signatures for introgressive gene flow. *Sci Adv* **4**,
522   eaap9873 (2018).

523 W. Bateson, *Materials for the Study of Variation, Treated with Special Regard to Discontinuity*
524   *in the Origin of Species* (Macmillan, London, 1894).

525 A. Berta, M. Churchill, R. W. Boessenecker, The Origin and Evolutionary Biology of
526   Pinnipeds: Seals, Sea Lions, and Walruses. *Ann. Rev. Earth. Plan. Sci.* **46**,
527   https://doi.org/10.1146/annurev-earth-082517-010009 (2018).

528 P. M. Butler, Studies of the mammalian dentition. Differentiation of the postcanine dentition.

529   *Proc Zool Soc London B* **109**, 1–36 (1939).

530   P. A. Corfman, R. M. Richart, Chromosomes of the ring seal. *Nature* **204**, 502–503 (1964).

531   L. Cruwys, A. Friday, Visible supernumerary teeth in pinnipeds. *Polar Rec.* **42**, 83–85 (2006).

532   I. L. Dryden, K. V. Mardia, *Statistical Shape analysis, with Applications in R* (John Wiley and
533   Sons, Chichester, 2016).

534   E.Y. Durand, N. Patterson, D. Reich, M. Slatkin, Testing for ancient admixture between closely
535   related populations. *Mol Biol Evol* **28**, 2239–2252 (2011).

536   J. Enk, A. Devault, R. Debruyne, C. E. King, T. Treangen, D. O'Rourke, S. L. Salzberg, D.
537   Fisher, R. MacPhee, H. Poinar, Complete Columbian mammoth mitogenome suggests
538   interbreeding with woolly mammoths. *Genome Biol.* **12**, R51 (2011).

539   V. Franco-Trecu, C. Abud, M. Feijoo, G. Kloetzer, M. Casacuberta, P. Costa-Urrutia, Sex
540   beyond species: the first genetically analyzed case of intergeneric fertile hybridization in
541   pinnipeds. *Evol. Dev.* **18**, 127–136 (2016).

542   G. J. Fraser, C. D. Hulsey, R. F. Bloomquist, K. Uyesugi, N. R. Manley, J. T. Streelman, An
543   ancient gene network is co-opted for teeth on old and new jaws. *PLoS Biol.* **7**, e31 (2009).

544   Q. Fu, M. Hajdinjak, O. T. Moldovan, S. Constantin, S. Mallick, P. Skoglund, N. Patterson, N.
545   Rohland, I. Lazaridis, B. Nickel, B. Viola, K. Prüfer, M. Meyer, J. Kelso, D. Reich, S.
546   Pääbo, An early modern human from Romania with a recent Neanderthal ancestor. *Nature*
547   **524**, 216–219 (2015).

548   T. L. Fulton, C. Strobeck, Multiple markers and multiple individuals refine true seal phylogeny
549   and bring molecules and morphology back in line. *Proc. R. Soc. B* **277**, 1065–1070 (2010).

550   S. Gerber, M. J. Hopkins, Mosaic heterochrony and evolutionary modularity: the trilobite genus

551 *Zacanthopsis* as a case study. *Evolution* **65**, 3241–3252 (2011).

552 H. T. Goodwin, Supernumerary teeth in Pleistocene, recent, and hybrid individuals of the

553 *Spermophilus richardsonii* complex (Sciuridae). *J. Mammal.* **79**, 1161–1169 (1998).

554 R. E. Green, J. Krause, A. W. Briggs, T. Maricic, U. Stenzel, M. Kircher, N. Patterson, H. Li,

555 W. Zhai, M. H.-Y. Fritz, N. F. Hansen, E. Y. Durand, A.-S. Malaspinas, J. D. Jensen, T.

556 Marques-Bonet, C. Alkan, K. Prüfer, M. Meyer, H. A. Burbano, J. M. Good, R. Schultz, A.

557 Aximu-Petri, A. Butthof, B. Höber, B. Höffner, M. Siegemund, A. Weihmann, C.

558 Nusbaum, E. S. Lander, C. Russ, N. Novod, J. Affourtit, M. Egholm, C. Verna, P. Rudan,

559 D. Brajkovic, Ž. Kucan, I. Gušic, V. B. Doronichev, L. V. Golovanova, C. Lalueza-Fox, M.

560 de la Rasilla, J. Fortea, A. Rosas, R. W. Schmitz, P. L. F. Johnson, E. E. Eichler, D. Falush,

561 E. Birney, J. C. Mullikin, M. Slatkin, R. Nielsen, J. Kelso, M. Lachmann, D. Reich, S.

562 Pääbo, A draft sequence of the Neandertal genome. *Science* **328**, 710–722 (2010).

563 D. M. Grossnickle, P. D. Polly, Mammal disparity decreases during the Cretaceous angiosperm

564 radiation. *Proc. R. Soc. B* **280**, 20132110 (2013). 10.1098/rspb.2013.2110

565 E. Harjunmaa, A. Kallonen, M. Voutilainen, K. Hämäläinen, M. L. Mikkola, J. Jernvall, On the

566 difficulty of increasing dental complexity. *Nature* **483**, 324–327 (2012).

567 E. Harjunmaa, K. Seidel, T. Häkkinen, E. Renvoisé, I. J. Corfe, A. Kallonen, Z.-Q. Zhang, A. R.

568 Evans, M. L. Mikkola, I. Salazar-Ciudad, O. D. Klein, J. Jernvall, Replaying evolutionary

569 transitions from the dental fossil record. *Nature* **512,** 44–48 (2014).

570 M. J. Hubisz, K. S. Pollard, A. Siepel, PHAST and RPHAST: phylogenetic analysis with

571 space/time models. *Brief Bioinform* **12**, 41–51 (2010).

572 J. Jernvall, Linking development with generation of novelty in mammalian teeth. *Proc. Natl*

573 *Acad. Sci. USA* **97**, 2641–2645 (2000).

574   J. Jernvall, I. Thesleff, Tooth shape formation and tooth renewal: Evolving with the same

575   signals. *Development* **139**, 3487–3497 (2012).

576   H. Jónsson, M. Schubert, A. Seguin-Orlando, A. Ginolhac, L. Petersen, M. Fumagalli, A.

577   Albrechtsen, B. Petersen, T. S. Korneliussen, J. T. Vilstrup, T. Lear, J. L. Myka, J.

578   Lundquist, D. C. Miller, A. H. Alfarhan, S. A. Alquraishi, K. A. S. Al-Rasheid, J.

579   Stagegaard, G. Strauss, M. Frost Bertelsen, T. Sicheritz-Ponten, D. F. Antczak, E. Bailey,

580   R. Nielsen, E. Willerslev, L. Orlando, Speciation with gene flow in equids despite extensive

581   chromosomal plasticity. *Proc. Natl. Acad. Sci. USA* **111**, 18655–18660 (2014).

582   M. Jussila, A. J. Aalto, M. S. Navarro, V. Shirokova, A. Balic, A. Kallonen, T. Ohyama, A. K.

583   Groves, M. L. Mikkola, I. Thesleff, Suppression of epithelial differentiation by Foxi3 is

584   essential for molar crown patterning. *Development* **142**, 3954–3963 (2015).

585   K. D. Kavanagh, A. R. Evans, J. Jernvall, Predicting evolutionary patterns of mammalian teeth

586   from development. *Nature* **449**, 427–432 (2007).

587   W. J. Kent, C. W. Sugnet, T. S. Furey, K. M. Roskin, T. H. Pringle, A. M. Zahler, D. Haussler,

588   The human genome browser at UCSC. *Genome Res.* **12**, 996–1006 (2002).

589   S. M. Kiełbasa, R. Wan, K. Sato, P. Horton, M. C. Frith, Adaptive seeds tame genomic

590   sequence comparison. *Genome Res* **21**, 487–493 (2011).

591   R. J. Kinsella, A. Kähäri, S. Haider, J. Zamora, G. Proctor, G. Spudich, J. Almeida-King, D.

592   Staines, P. Derwent, A. Kerhornou, P. Kersey, P. Flicek, Ensembl BioMarts: a hub for data

593   retrieval across taxonomic space. *Database* 2011 (2011).

594   C. P. Klingenberg, Evolution and development of shape: integrating quantitative approaches.

595   *Nat. Rev. Genet.* **11**, 623–635 (2010).

596   C. P. Klingenberg, MorphoJ: an integrated software package for geometric morphometrics. *Mol*

597   *Ecol Resour* **11**, 353–357 (2011).

598   T. S. Korneliussen, A. Albrechtsen, R. Nielsen, ANGSD: Analysis of next generation
599   sequencing data. *BMC Bioinformatics* **15**, 356 (2014).

600   K. M. Kovacs, C. Lydersen, M. O. Hammill, B. N. White, P. J. Wilson, S. Malik, A harp seal X
601   hooded seal hybrid. *Mar. Mam. Sci.* **13**, 460–468 (1997).

602   V. Kumar, F. Lammers, T. Bidon, M. Pfenninger, L. Kolter, M. A. Nilsson, A. Janke, The
603   evolutionary history of bears is characterized by gene flow across species. *Sci. Rep.* **7**,
604   46487 (2017).

605   K. Kupczik, A. Cagan, S. Brauer, M. S. Fischer, The dental phenotype of hairless dogs with
606   FOXI3 haploinsufficiency. *Sci Rep* **7**, 5459 (2017).

607   S. Lamichhaney, F. Han, M. T. Webster, L. Andersson, B. R. Grant, P. R. Grant, Rapid hybrid
608   speciation in Darwin's finches. *Science* **359**, 224–228 (2018).

609   H. Li, R Durbin, Fast and accurate short read alignment with Burrows-Wheeler Transform.
610   *Bioinformatics* **25**, 1754–1760 (2009).

611   Z.-X. Luo, Transformation and diversification in early mammal evolution. *Nature* **450**, 1011–
612   1019 (2007).

613   E. Lönnberg, A hybrid between gray seal, *Halichoerus grypus* Nils. and Baltic ringed seal,
614   *Phoca hispida annellata* Nils. *Arkiv. för Zoologi* **21A**, 1–8 (1929).

615   A. Löytynoja, A. J. Vilella, N. Goldman, Accurate extension of multiple sequence alignments
616   using a phylogeny-aware graph algorithm. *Bioinformatics* **28**, 1684–1691 (2012).

617   J. Mallet, Hybrid speciation. *Nature* **446**, 279–283 (2007).

618   M. Martin, Cutadapt removes adapter sequences from high-throughput sequencing reads.

619   *EMBnet.journal* **17**, 10–12 (2011).

620   M. Martinón-Torres, X. Wu, J. M. Bermúdez de Castro, S. Xing, W. Liu, *Homo sapiens* in the

621   Eastern Asian Late Pleistocene. *Curr. Anthropol.* **58** (supp. 17), S434–S448 (2017).

622   A. McKenna, M. Hanna, E. Banks, A. Sivachenko, K. Cibulskis, A. Kernytsky, K. Garimella,

623   D. Altshuler, S. Gabriel, M. Daly, M. A. DePristo, The Genome Analysis Toolkit: a

624   MapReduce framework for analyzing next-generation DNA sequencing data. *Genome Res.*

625   **20**, 1297–303 (2010).

626   M. Meyer, M. Kircher, M.-T. Gansauge, H. Li, F. Racimo, S. Mallick, J. G. Schraiber, F. Jay,

627   K. Prüfer, C. de Filippo, P. H. Sudmant, C. Alkan, Q. Fu, R. Do, N. Rohland, A. Tandon,

628   M. Siebauer, R. E. Green, K. Bryc, A. W. Briggs, U. Stenzel, J. Dabney, J. Shendure, J.

629   Kitzman, M. F. Hammer, M. V. Shunkov, A. P. Derevianko, N. Patterson, A. M. Andrés, E.

630   E. Eichler, M. Slatkin, D. Reich, J. Kelso, S. Pääbo, A high-coverage genome sequence

631   from an archaic Denisovan individual. *Science* **338**, 222–226 (2012).

632   E. H. Miller, H.-C. Sung, V. D. Moulton, G. W. Miller, J. K. Finley, G. B. Stenson, Variation

633   and integration of the simple mandibular postcanine dentition in two species of phocid seal.

634   *J. Mamm.* **88**, 1325–1334 (2007).

635   K. Nyakatura, O. R. P. Bininda-Emonds, Updating the evolutionary history of Carnivora

636   (Mammalia): a new species-level supertree complete with divergence time estimates. *BMC*

637   *Biol.* **10**, 12 (2012).

638   L. F. Pallares, L. M. Turner, D. Tautz, Craniofacial shape transition across the house mouse

639   hybrid zone: implications for the genetic architecture and evolution of between-species

640   differences. *Dev. Genes Evol.* **226**, 173-186 (2016).

641   E. Paradis, J. Claude, K. Strimmer, APE: analyses of phylogenetics and evolution in R

642   language. *Bioinformatics* **20**, 289–290 (2004).

643   E. Pennisi, Shaking up the tree of life. *Science* **354**, 817–821 (2016).

644   P. D. Polly, A. V. Polyakov, V. B. Ilyashenko, S. S. Onischenko, T. A. White, N. A.

645   Shchipanov, N. S. Bulatova, S. V. Pavlova, P. M. Borodin, J. B. Searle, Phenotypic

646   variation across chromosomal hybrid zones of the common shrew (*Sorex araneus*) indicates

647   reduced gene flow. *PLoS One* **8**, e67455 (2013).

648   R Core Team, *R: A language and environment for statistical computing* (R Foundation for

649   Statistical Computing, Vienna, 2009).

650   E. Renvoisé, K. D. Kavanagh, V. Lazzari, T. J. Häkkinen, R. Rice, S. Pantalacci, I. Salazar-

651   Ciudad, J. Jernvall, Mechanical constraint from growing jaw facilitates mammalian dental

652   diversity. *Proc. Natl Acad. Sci. USA* **114**, 9403–9408 (2017).

653   I. Salazar-Ciudad, J. Jernvall, A computational model of teeth and the developmental origins of

654   morphological variation. *Nature* **464**, 583–586 (2010).

655   Y. Savriama, C. P. Klingenberg, Beyond bilateral symmetry: geometric morphometric methods

656   for any type of symmetry. *BMC Evol Biol* **11,** 280 (2011).

657   S. Schlager, "Morpho and Rvcg – Shape Analysis in R: R-Packages for Geometric

658   Morphometrics, Shape Analysis and Surface Manipulations" in *Statistical Shape and*

659   *Deformation Analysis,* G. Zheng, S. Li, G. Szekely Eds. (Academic Press, 2017) pp. 217–

660   256.

661   O. Seehausen, Hybridization and adaptive radiation. *Trends in Ecol. Evol.* **19**, 198–207 (2004).

662   Q. R. Shurtliff, Mammalian hybrid zones. *Mamm. Rev.* **43**, 1–21 (2013).

663   L. Skotte, T. S. Korneliussen, A. Albrechtsen, Estimating individual admixture proportions from

664   next generation sequencing data. *Genetics* **195**, 693–702 (2013).

665   A. Stamatakis, RAxML-VI-HPC: maximum likelihood-based phylogenetic analyses with

666   thousands of taxa and mixed models. *Bioinformatics* **22**, 2688–2690 (2006).

667   T. Stringell, D. Hill, D. Rees, F. Rees, P. Rees, G. Morgan, L. Morgan, C. Morris, Predation of

668   harbour porpoises (*Phocoena phocoena*) by grey seals (*Halichoerus grypus*) in Wales.

669   *Aquat. Mamm.* **41**, 188–191 (2015).

670   I. Tattersall, J. H. Schwartz, Morphology, paleoanthropology, and Neanderthals. *Anat. Rec.* **253**,

671   113-117 (1998).

672   E. Trinkaus, European early modern humans and the fate of the Neandertals. *Proc. Natl Acad.*

673   *Sci. USA* **104**, 7367–7372 (2007).

674   E. Trinkaus, O. Moldovan, Ş. Milota, A. Bîlgăr, L. Sarcina, S. Athreya, S. E. Bailey, R.

675   Rodrigo, G. Mircea, T. Higham, C. B. Ramsey, J. van der Plicht, An early modern human

676   from the Pestera cu Oase, Romania. *Proc. Natl Acad. Sci. USA* **100**, 11231–11236 (2003).

677   P. Ukkonen, K. Aaris-Sørensen, L. Arppe, L. Daugnora, A. Halkka, L. Lõugas, M. J. Oinonen,

678   M. Pilot, J. Storå, An Arctic seal in temperate waters: History of the ringed seal (*Pusa*

679   *hispida*) in the Baltic Sea and its adaptation to the changing environment. *Holocene* **24**,

680   1694–1706 (2014).

681   M. Valtonen, J. U. Palo, M. Ruokonen, M. Kunnasranta, T. Nyman, Spatial and temporal

682   variation in genetic diversity of an endangered freshwater seal. *Conserv. Genet.* **13**, 1231–

683   1245 (2012).

684   A. van Neer, L. F. Jensen, U. Siebert, Grey seal (*Halichoerus grypus*) predation on harbour

685   seals (*Phoca vitulina*) on the island of Helgoland, Germany. *J. Sea Res.* **97**, 1–4 (2015).

686   L. Van Valen, Growth fields in the dentition of *Peromyscus*. *Evol. Int. J. Org. Evol.* **16**, 272–

687   277 (1962).

688   C. M. Vella, L. M. Shelton, J. J. McGonagle, T. W. Stanglein, *Robinson's Genetics for Cat*

689   *Breeders and Veterinarians* (Butterworth-Heinemann Ltd., Oxford, ed. 4, 1999).

690   K. A. Warren, T. B. Ritzman, R. A. Humphreys, C. J. Percival, B. Hallgrímsson, R.R.

691   Ackermann, Craniomandibular form and body size variation of first generation mouse

692   hybrids: A model for hominin hybridization. *J. Hum. Evol.* **116**, 57–74 (2018).

693   K. Wecek, S. Hartmann, J. L. A. Paijmans, U. Taron, G. Xenikoudakis, J. A. Cahill, P. D.

694   Heintzman, B. Shapiro, G. Baryshnikov, A. N. Bunevich, J. J. Crees, R. Dobosz, N.

695   Manaserian, H. Okarma, M. Tokarska, S. T. Turvey, J. M. Wójcik, W. Żyła, J. M. Szymura,

696   M. Hofreiter, A. Barlow, Complex admixture preceded and followed the extinction of

697   wisent in the wild. *Mol. Biol. Evol.* **34**, 598–612 (2017).

698   D. F. Wiley, N. Amenta, D.A. Alcantara, D. Ghosh, Y.J. Kil, E. Delson, W. Harcourt-Smith,

699   F.J. Rohlf, K. St John, B. Hamann, Evolutionary morphing. *Proceedings of the IEEE*

700   *Visualization* 2005 *(VIS'05)*, 431–438 (2005).

701   S. C. Wilson, Attempted mating between a male gray seal and female harbor seal. *J. Mammal.*

702   **56**, 531–534 (1975).

703   A. Yates, K. Beal, S. Keenan, W. McLaren, M. Pignatelli, G. R. S. Ritchie, M. Ruffier, K.

704   Taylor, A. Vullo, P. Flicek, The Ensembl REST API: Ensembl data for any language.

705   *Bioinformatics* **31**, 143–145 (2014).

706   H. Zhao, Z, Sun, J. Wang, H. Huang, J.-P. Kocher, L. Wang, CrossMap: a versatile tool for

707   coordinate conversion between genome assemblies. *Bioinformatics* **30**, 1006–1007 (2013).
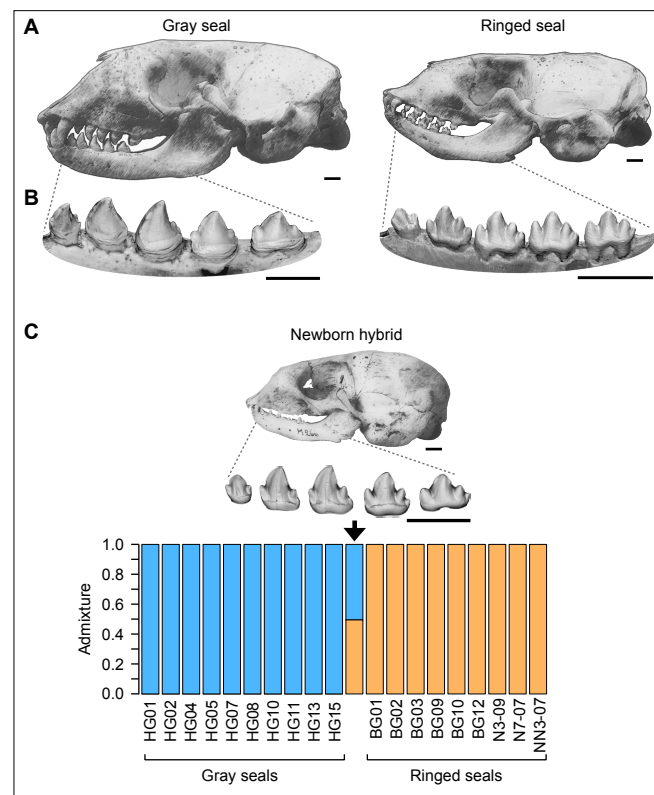
708

709

710

Figure 1. Gray and ringed seal cranio-dental morphologies show at least genus-level differences and genetic data validates the hybrid specimen. (A) The gray seal skull has a prominent snout with a straight profile whereas the overall cranial morphology of ringed seals is relatively gracile. (**B**) The gray seal lower postcanines have robust, fang-shaped central cusps with small and variably present accessory cusps. There is a marked gradation of tooth shapes along the jaw, and gray seal teeth are approximately 40% larger (anteroposteriorly) than ringed seal teeth. The ringed seal lower postcanines have typically four slender cusps on the four large postcanines of the lower jaw. Upper teeth show comparable but less disparate differences in cusp number. Gray seals have pronounced sexual dimorphism and the skull illustrations are of females. Postcanine dentitions, showing obliquely lingual views, have no marked sexual dimorphism. **(C)** The hybrid specimen is a newborn skull and mandible with erupting, but fully formed teeth. Genetic analysis from hybrid dental pulp shows close to 50% admixture between gray (50.51%) and ringed (49.49%) seals. Analysis shown (K=2) was performed using NGSadmix of ANGSD with 3.6 million markers (see Materials and Methods). Scale bars, 10 mm.
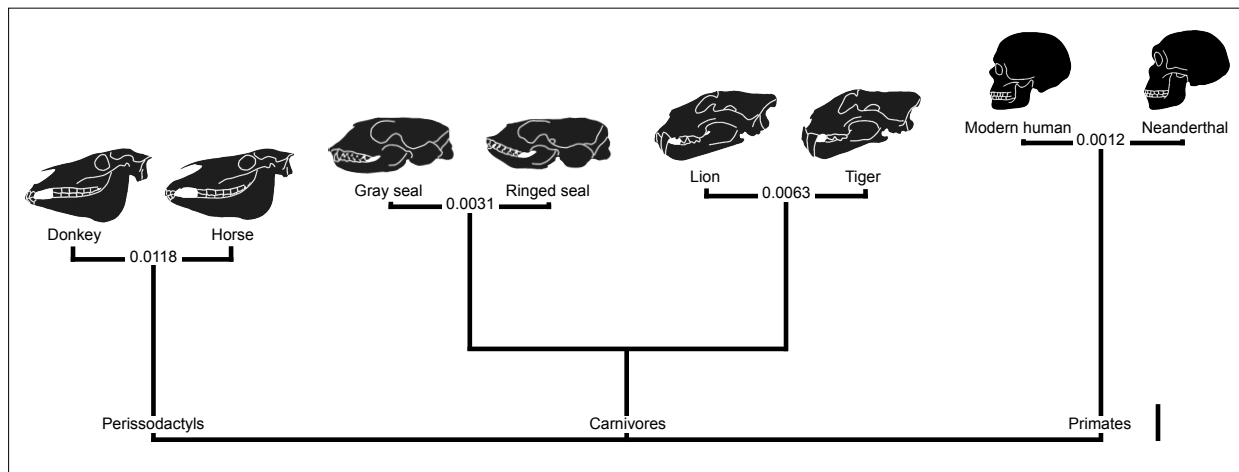
726

727

728

Figure 2. Bracketing the genetic distance of gray and ringed seals with other hybridizing taxa. Lion-tiger and donkey-horse distances (substitutions per fourfold degenerate site) are longer, and human-Neanderthal distance is shorter than the gray-ringed seal distance. Of the hybridizing species pairs, only gray and ringed seals are in different genera, and have pronounced differences in both dental and cranial morphologies. Pairwise distances (T92 model) and a phylogenetic tree were built using fourfold degenerate sites of 4,045 orthologous genes. For details and all the distances, see Materials and Methods and Table 1. Scale bar, 0.02 substitutions per ffd. The crania shown are not to scale. The horse cranium is of *E. f. przewalskii.*
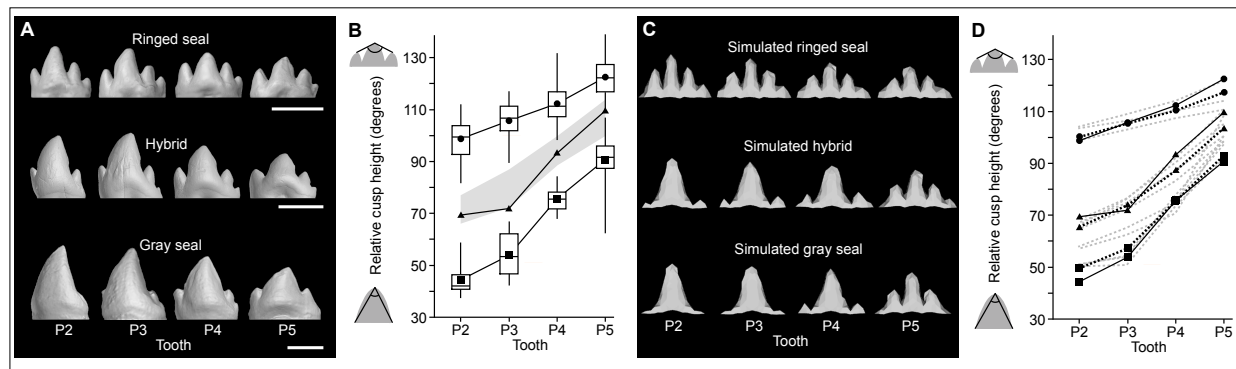
738

739

740

Figure 3. Teeth of the hybrid are morphologically and developmentally intermediate. (A) The hybrid has the large central cusps of the gray seal together with relatively prominent accessory cusps reminiscent of the ringed seals. (**B**) The top-cusp angle measure shows that the hybrid teeth (triangles) are intermediate between the ringed (circles, n = 43, 50, 49, and 49 for P2, P3, P4, and P5) and gray (squares, n = 41, 44, 39, and 53 for P2, P3, P4, and P5) seals with no overlap in P2 to P4, and marginal overlap with ringed seal teeth in P5. Gray area marks 80% of the angles averaged between each gray-ringed seal pair (see Figure supp. 2). Boxes enclose 50% of observations; the median and mean are indicated with a horizontal bar and circle or square, respectively, and whiskers denote range. (**C**) Simulated ringed and gray seal tooth rows that were manually matched with mean real shapes. The tooth row of the simulated hybrid was obtained by averaging the values of the parents. (**D**) The top-cusp angle measure shows that the average-value-simulated hybrid teeth (triangles, black dashed line) are intermediate between the simulated gray (squares, black dashed line) and ringed (circles, black dashed line) seal teeth, and comparable to the real hybrid teeth (triangles, black solid line). Gray dashed lines show hybrid simulation in which maternal or paternal values were tested for each parameter (Figure supp. 3, Table supp. 8). Teeth have been mirrored if needed to show left buccal views. Scale bars, 5 mm.
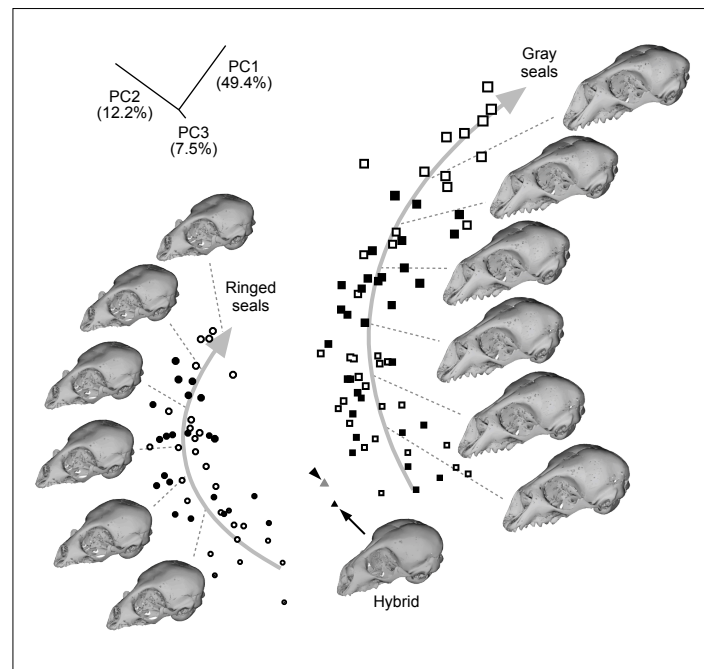
758

759

760

Figure 4. Ringed and gray seal crania are distinct at the birth and the hybrid is intermediate between the species. A geometric morphometric analysis shows the developmental trajectories from newborn to adult ringed (circles, n = 49) and gray (squares, n = 66) seals for the first three components (PCA). Arrows display developmental trajectories obtained by multivariate quadratic regressions of shape onto centroid size. The symbol size represents the relative centroid size of the crania and open symbols are male, black female. The larger size and more pronounced nasal region of gray seals are further developed in males. Arrowhead denotes the geometric mean calculated using the youngest ringed (n = 11) and gray seal (n = 11) crania. See Figure supp. 4, 5 and Materials and Methods.
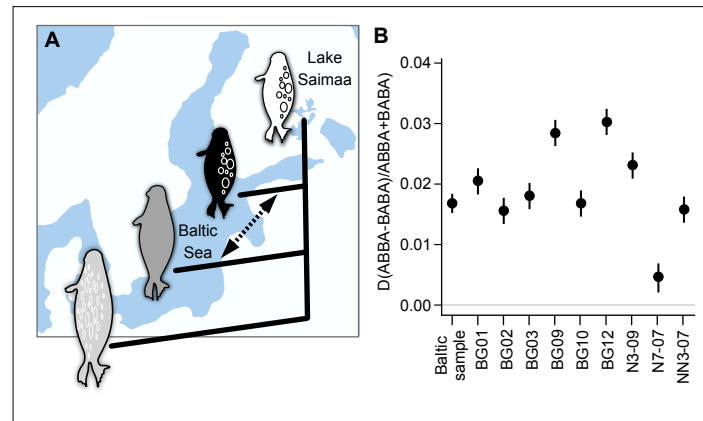
770

771

772

773

Figure 5. **Introgression analysis suggests interbreeding between Baltic gray and ringed seals in the wild. (A)** Saimaa ringed seals (white) have been landlocked in the Lake Saimaa, Finland for 9,500 years, providing a suitable comparison for Baltic ringed seals (black) and gray seals (gray). Outgroup was the Weddell seal (light gray). (**B**) Positive D-statistic values, calculated using D(Saimaa ringed seal, Baltic ringed seal; Baltic gray seal, Weddell seal) indicate gene flow between Baltic gray and ringed seals (arrow in A). Although the introgression and Z-scores vary between the individuals, all but one individual (N7-07) were $p < 0.0001$ (Table supp. 10 and Materials and Methods). Whiskers denote one standard error.

782

783

784 **Table 1.** Genetic distances between hybridizing species (substitutions per fourfold degenerate
785 site).

	Human	Neanderthal	Tiger	Lion	Horse	Donkey	Ringed seal
Neanderthal	0.0012						
Tiger	0.2596	0.2596					
Lion	0.2599	0.2598	0.0063				
Horse	0.2369	0.2368	0.2164	0.2165			
Donkey	0.2366	0.2365	0.2159	0.2160	0.0118		
Ringed seal	0.2539	0.2539	0.1541	0.1542	0.2084	0.2079	
Gray seal	0.2540	0.2539	0.1544	0.1544	0.2086	0.2082	0.0031

786   Based on 1,526,260 codons, 623,391 fourfold degenerate sites, and 4,045 orthologous genes.

787